Automotive CMOS Image Sensor Family with 2.1µm LFM Pixel, 150 dB Dynamic Range and High Temperature Stability

Manuel Innocent[1], Sergey Velichko[2], Grady Anderson[2], Jeff Beck[3]*, Augie Hernandez[3], Barry Vanhoff[3], Chris Silsby[3], Anirudh Oberoi[4], Gurvinder Singh[4], Sundaraiah Gurindagunta[4], Ravi Mahadevappa[4], Maheedhar Suryadevara[4], Darryl Perks[5], Benjamin Hung[7], Daniel Tekleab[7], Tomas Geurts[1]*, Michael Guidash[7] and Vladi Korobov[7]

onsemi, [1] Schaliënhoevedreef 20B, 2800 Mechelen, Belgium, Manuel.Innocent@onsemi.com, tel +32 15 446 390
[2] Boise ID, USA [3] Corvallis OR, USA [4] Bangalore, India [5] Bracknell, UK [7] Sunnyvale CA, USA
*contributed while previously at onsemi

This paper presents an image sensor family for automotive applications. The sensors have a 2.1 µm pixel with overflow to a low gain capacitor, a triple gain readout and light flicker mitigation (LFM). The single exposure (flicker free) dynamic range is 110 dB and the SNR stays above 25 dB at each of the transition points up to 125°C. By adding a second exposure the dynamic range reaches up to 150 dB. The family currently consists of an 8.3 MP and a 3 MP sensor. More resolutions will be added.

Motivation

The most common techniques for extending the dynamic range of an image sensor are multiple exposure [1-3], dual photo diode [4-6] and overflow [7-11] or a combination of these. Multi exposure combines images with different integration times which causes artefacts on moving objects or pulsed light sources. The case with pulsed light sources is of particular interest for automotive applications as traffic signs and taillights of cars often use pulsed LEDs. The dual photo diode approach allows for a high flicker free dynamic range but loses sensitivity on the large photo diode, does not scale well to a smaller pitch and the consistency of color and MTF between the diodes is an issue. Therefore, our sensors use overflow from a single photo diode onto a very large capacitor. The sensors aim at automotive applications both in pixel specifications and in sensor features. A high single exposure dynamic range and good performance at high temperature are two key elements. A second short integration time can increase the dynamic range up to 150 dB. Flickering light sources will no longer cause artefacts when the long integration time has sufficient dynamic range to capture them unsaturated. 110 dB covers almost all use cases.

Test chip characterization data and initial data from the 8.3 MP product were presented in [11]. This paper presents characterization data over temperature from the product and focusses on one particularly challenging aspect: the trade off between DSNU, full well charge and blooming at high temperature.

Pixel design, operation, and performance

Figure 1 shows the pixel schematic. It is an overflow pixel with an additional dual conversion gain (DCG) transistor for a medium gain. The pixel combines overflow to a low gain capacitor with a triple gain readout. The low gain capacitor is a trench MiM that allows for a full well charge of 600 ke⁻. This high capacitance results in a substantial read noise due to its kT/C noise and a degraded input referred read noise because of the low charge to voltage conversion gain. This read noise is the dominant noise contribution on the low gain read up to high temperature. The floating diffusion DSNU is highly optimized and at 10 ms integration time it only dominates over the read noise at the 125 °C data point.

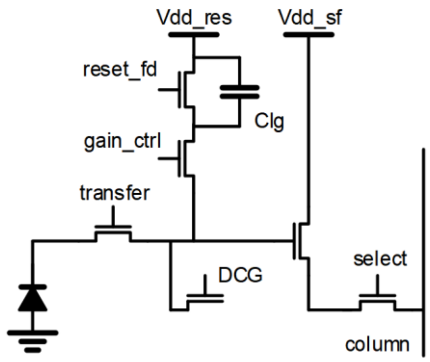

Figure 1: Schematic of the pixel. Clg is an MiM overflow capacitor. The dual conversion gain transistor (DCG) can add capacitance to the FD for the medium gain.

Figure 2 shows a simplified timing diagram for the operation with a triple gain T1 read and a low gain T2 read. Each of the three T1 reads has a response starting from the origin. Signal charge is not reset in between the reads. The gain is lowered going to the next read and more signal charge is added. Eventually the low gain read contains all charge from the PD and the overflow capacitor. The high gain PD read uses correlated double sampling and 4x analog gain to minimize noise. The other reads are double sampling reads.

Figure 3 shows the measured SNR for multiple temperatures. The transition SNRt stays around 30 dB at each of the transitions up to 100°C. At 125 °C the SNRt at the transition between the PD and the overflow read still maintains a level around 25 dB. The SNRt at the transition between the T1 overflow read and T2 does not change significantly with temperature. It is mainly a function of the integration time ratio. This ratio can be chosen at runtime and trades SNRt for total DR. The figure shows the curves for a ratio of 70 which results in an SNRt slightly below 30 dB and a total DR of 146 dB. When the focus is on higher SNRt a ratio of e.g. 44 results in an SRNt of 32 dB and a total DR of 143 dB. With focus on higher DR e.g. a ratio of 100 results in an SNRt of 26 dB and a total DR of 150 dB.

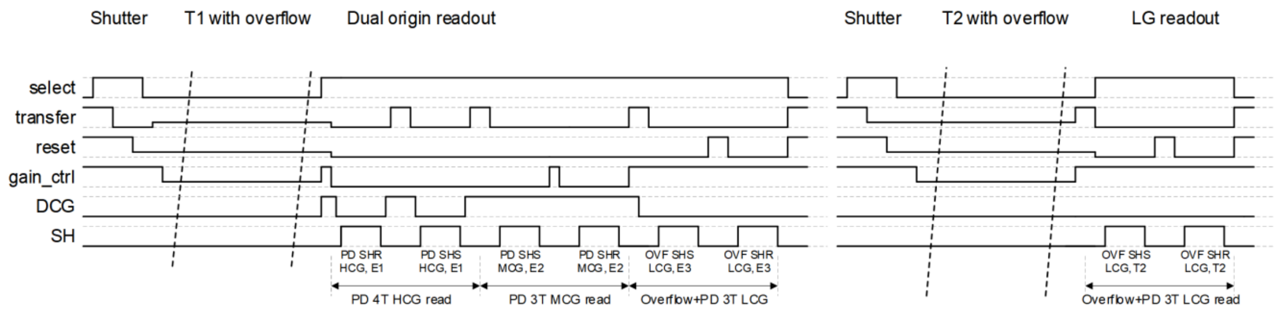

Figure 2: Timing diagram of the overflow T1 with triple gain origin mode read and overflow T2 with low gain read. The overflow T1 is also referred to as a "Super-Exposure" (SE) as it combines signals from multiple in pixel readout gains and covers a very wide DR.

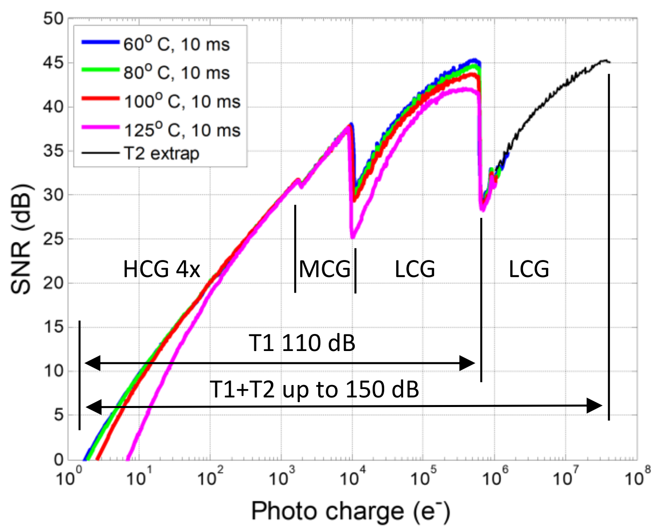

Figure 3: Measured SNR of the 8.3 MP sensor as a function of exposure. Clear pixel, red light spectrum. Super-Exposure T1 and low gain T2, T1/T2=70. The T2 range beyond the maximum power of the available light source is extrapolated form the T1 overflow measurement.

These SNR curves show that these devices are designed for high temperature operation. The performance at 60 °C and 80 °C is almost indistinguishable and at 100 °C there is only a minor degradation of SNR1. At 125 °C the SNR1 degrades noticeable due to increased PD DSNU but is on par with our same pixel size multi-exposure sensor which is state of the art and has a much simpler pixel operation. The PD DSNU has improved from the early samples by finetuning the blooming prevention mechanism. This has a trade-off that shows at the high end of the T1 overflow read where the peak SNR is a little lower at 125 °C. This is not due to DSNU as that would have no impact at such large signals. At very high temperature the sensor operates at the onset of blooming which results in increased PRNU. This is not an issue as the SNR is still over 40 dB. Also, the SNRt is hardly changing with temperature up to 100 °C since it is read noise dominated. Only at 125 °C FD DSNU dominates over the read noise.

Blooming optimization

The optimization for blooming free operation at high temperature was a very challenging aspect of this development. The pixel is processed with a partial backside deep-trench isolation (BDTI). This improves the optical properties, but unlike a full DTI does not prevent blooming between pixels. Blooming is controlled by a sufficiently conductive overflow path.

Usually blooming occurs when the photo diode is full and additional photo generated charge spills over to a neighboring pixel. In an overflow pixel charge overflows to the low gain capacitor at this point. This is normal operation. When the overflow capacitor also saturates charge must overflow over the reset_fd device to the supply. This proved to be the most critical condition for the optimization. A "waterfall" must be created from the PD to the FD, Clg and Vdd_res. Setting the low-level voltages on transfer, gain_ctrl or reset_fd higher than strictly needed will reduce the available swing (full well charge) and increase DSNU at the respective location. Similarly, a higher Vdd_res can reduce blooming and increase available swing but will also increase DSNU. The transfer gate turned out to be the most critical location for controlling the blooming even though the blooming only occurs when Clg saturates.

In the early samples the blooming was controlled by pixel timing and increased low level voltages. That works well to control the blooming, but it increases the PD DNSU which is a problem at high temperature. This was improved by optimizing the layout and implant scheme of the buried channel "anti-blooming" overflow path under the transfer gate such that it conducts sufficiently while keeping the transfer gate in the "off" state. Figure 4 shows a drawing of the buried channel path under the transfer gate which can be thought off as a grounded JFET in parallel to the transfer gate. The operation depends on the sub-threshold current of the device which turned out to be very sensitive to layout, not only of the transfer gate itself, but also nearby implants like isolations. Maximizing the width of the anti-bloom path and removing neighboring isolation implants maximized the current handling without sacrificing too much PD full well charge.

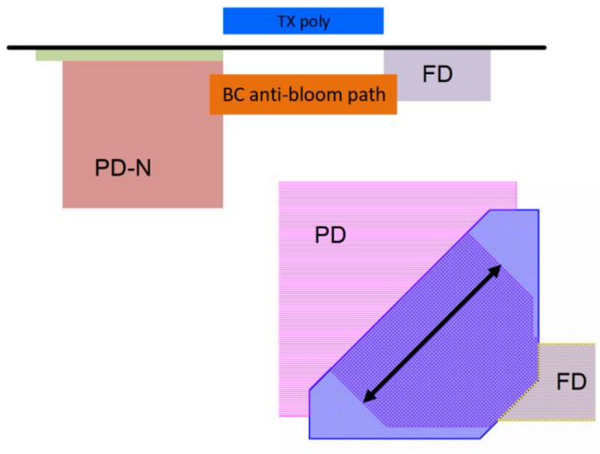

Figure 4: Concept drawing of the buried channel anti-bloom path. This path allows charge to overflow from the photo diode to the floating diffusion while the transfer gate is kept in the "off" state. The arrow in the layout view indicates the width of the anti-bloom path under the transfer gate.

Blooming PRNU metric

The trade-off between full well charge, DNSU and blooming requires a good way to quantify blooming. This led to the introduction of a new metric for blooming in the overflow regime: blooming PRNU

Traditionally, blooming is quantified by a slope change in the response of the slow color channel after saturation of the dominant color channel. However, this metric does not correlate well with image quality. Even without a slope change the image quality can be degraded by outlier pixels that are already blooming and can show up as colored spots. Therefor we introduce a new metric for blooming based on fixed pattern noise: blooming PRNU. Blooming PRNU quantifies how the fixed pattern noise in the slow channel scales with the illumination of the dominant channel.

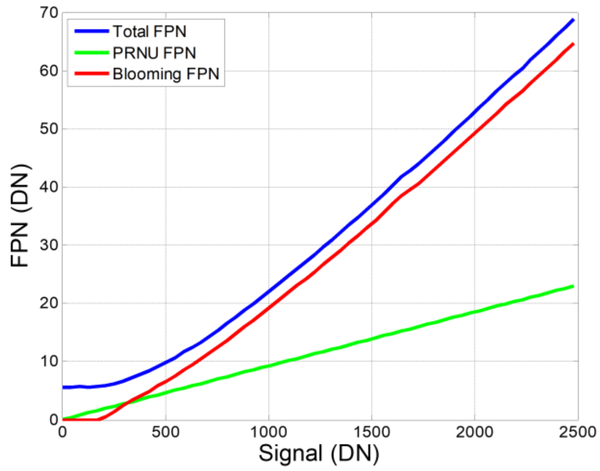

Figure 5: FPN contributions on the slow color channel (red pixel, cyan light spectrum, RGGB CFA) as a function of slow channel signal. Example sensor with blooming at 125 °C. The red curve is the blooming FPN which scales with the (extrapolated) dominant channel signal (green pixel).

There are a few caveats: not all fixed pattern noise in the slow channel is due to blooming and the dominant color channel is saturated in the region of interest so an extrapolated value must be used. The fixed pattern noise in the slow channel is the sum of the dark FPN (including dark current non-uniformity), the PRNU of the response of the slow channel itself and the "blooming FPN". Figure 5 shows an example of the FPN contributions of the slow channel for a sensor with some blooming. Blooming is measured with cyan light to excite the blue, green and/or clear color channels. The red color channel is the victim in which blooming is measured. These measurements are done at 125 °C since this is the worst case.

The blooming FPN of the slow channel scales with the (extrapolated) response of the dominant color channel. Hence, the blooming PRNU is given by:

$$Blooming\ PRNU = \frac{\sqrt{FPN^2 - (dark\ FPN)^2 - PRNU^2}}{extrapolated\ dominant\ channel\ response}$$

Figure 6 shows the blooming PRNU for several test chip and product samples with two types of CFA. The blooming PRNU threshold for excellent image quality is around 1%. The product is with both types of CFA well below this 1% at 125 °C.

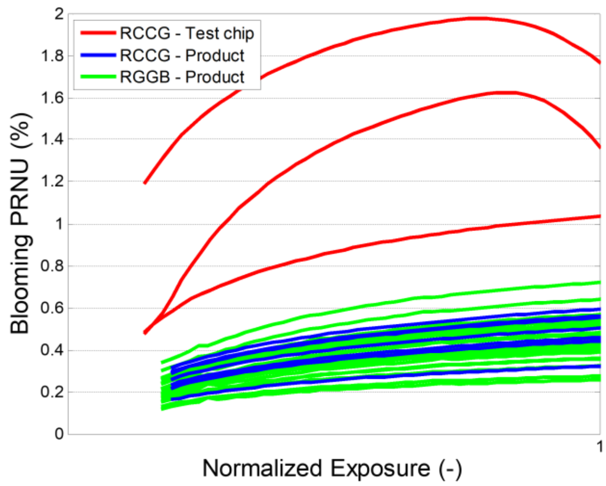

Figure 6: Blooming PRNU at 125 °C as a function of normalized exposure for some example pixel types from the test chip and multiple samples of the product. The exposure is normalized to the maximum cyan output power of the light source. This oversaturates the dominant channel by 4-6x depending on the CFA.

Discussion

The sensors provide 110 dB of single exposure dynamic range and up to 150 dB of total dynamic range with two exposures. The single exposure dynamic range is covered by a long T1 integration time of e.g. 10 ms. It has some motion blur which is inevitable with a long integration time, but it does not have motion artefacts due to combining data from several time shifted integration times. More importantly, in case of flickering light sources like LED's, the long integration time will capture at least one light pulse so that light source is never perceived as "off" [10]. At an integration time of 10 ms, the 600 ke^- FWC is sufficient to capture almost all automotive LED flickering sources without saturation. This is important for correctly capturing traffic signs and traffic lights. The dynamic range between 110 dB and 150 dB is covered by a second (very short) integration time. This T2 in the sub-millisecond range will mainly capture non flickering highlights like the sun and its specular reflections.

The total dynamic range of 150 dB is sufficient to simplify the camera exposure control. In most practical situations the integration time can be fixed. This reduces the system latency since the exposure control does not need to settle after a change in the scene.

The sensors have dual outputs with windowing and scaling. This allows combining an advanced driver-assistance system (ADAS) camera and viewing camera into one device, reducing system cost. A typical use case for the 8.3 MP sensor is the output of a full resolution 8.3 MP image for ADAS combined with a lower resolution (e.g. 2 MP) for viewing applications.

Table I summarizes the sensor properties and finally figure 7 illustrates the image quality in two extreme illumination cases.

Optical format	1/3.7" (3 MP), 1/1.8" (8.3 MP)
Pixel array	1920 (H) x 1536 (V) = 3 MP 3840 (H) x 2160 (V) = 8.3 MP
Color Filter Array	RGGB, RCCB, RYYCy
Pixel pitch	2.1 µm
Linear Full well	1.5 ke^- (E1 at 4x gain), 10 ke^- (E2), 600 ke^- (E3)
Read noise @ 80ºC	180 µV (E1), 2 mV (E2), 520 µV (E3)
Single exposure DR	110 dB (SNR1 based at 80 °C)
Total DR (T1+T2)	150 dB (for T1/T2=100)
Transition SNRt	30 dB at 80°C, 25 dB at 125°C
Max frame rate (8.3 MP)	45 fps T1+T2 at 26 bit companded to 16 60 fps T1 at 20 bit companded
Supply voltage	2.8 V, 1.8 V

Table I. Sensor properties and performance

Conclusion

Every aspect of this sensor family is designed with automotive applications in mind. Both the feature set and pixel performance aim at reducing the system complexity. Good high temperature performance and an extended flicker free and total dynamic range are key for obtaining high safety levels.

Up to 80°C the performance is almost indistinguishable from room temperature and at 100°C there is only a very minor increase of SNR1. Even at 125°C, which most competitors don't report, good image quality is maintained with an SNRt above 25 dB at each of the transitions.

References

[1] O. Yadid-Pecht and E. Fossum, "Wide Intrascene Dynamic Range CMOS APS Using Dual Sampling", IISW 1997.

[2] J. Solhusvik et al., "A 1280x960 3.75 µm pixel CMOS imager with Triple Exposure HDR", IISW 2009.

[3] S. Velichko et al., "140 dB Dynamic Range Sub-electron Noise Floor Image Sensor", IISW 2017.

[4] M.Innocent et al., "Pixel with nested photo diodes and 120 dB single exposure dynamic range", IISW 2019.

[5] Y. Sakano et al., "A 132 dB Single-Exposure-Dynamic-Range CMOS Image Sensor with High Temperature Tolerance", ISSCC, pp. 105–107, Feb. 2020.

[6] Y. Oh et al., "A 140 dB Single-Exposure Dynamic-Range CMOS Image Sensor with In-Pixel DRAM Capacitor", IEDM 2022

[7] N. Akahane et.al. "A sensitivity and linearity improvement of a 100-dB dynamic range CMOS image sensor using a lateral overflow integration capacitor", in IEEE Journal of Solid-State Circuits, vol. 41, no. 4, pp. 851-858, April 2006.

[8] Y. Fujihara et al., "An Over 120 dB Single Exposure Wide Dynamic Range CMOS Image Sensor With Two-Stage Lateral Overflow Integration Capacitor", Electron Devices IEEE Transactions on, vol. 68, no. 1, pp. 152-157, 2021.

[9] T. Geurts et al., "A 98 dB Linear Dynamic Range, High Speed CMOS Image Sensor", IISW 2017.

[10] M. Oh et al., "3.0 µm Backside illuminated, lateral overflow, high dynamic range, LED flicker mitigation image sensor", IISW 2019.

[11] M. Innocent et al., "Automotive 8.3 MP CMOS Image Sensor with 150 dB Dynamic Range and Light Flicker Mitigation," IEDM 2021.

Figure 7: Outdoor images with local tone mapping of the 3MP sensor.
Left: 2 ms integration time with direct sun light. Right: 30 ms integration time on a moonless night.